

Article

Matrix Methods for Solving Hartree-Fock Equations in Atomic Structure Calculations and Line Broadening

Thomas Gomez ^{1,*} , Taisuke Nagayama ¹, Dave Kilcrease ², Stephanie Hansen ¹, Mike Montgomery ³, and Don Winget³

¹ Sandia National Laboratories

² Los Alamos National Laboratory

³ University of Texas at Austin

* Correspondence: thogome@sandia.gov

Abstract: Atomic structure of N-electron atoms is often determined using the Hartree-Fock method, which is an integro-differential equation. The exchange term of the Hartree-Fock equations is usually treated as an inhomogeneous term of a differential equation, or with a local density approximation. This work uses matrix methods to solve for the Hartree-Fock equations, rather than the more commonly-used shooting method to integrate an inhomogeneous differential equation. It is well known that a derivative operator can be expressed as a matrix made of finite-difference coefficients; energy eigenvalues and eigenvectors can be obtained by using computer linear-algebra packages. We extend the same technique to integro-differential equations, where a discretized integral can be written as a sum in matrix form. This method is compared against experiment and standard atomic structure calculations. We also can use this method for free-electron wavefunctions. This technique is important for spectral line broadening in two ways: improving the atomic structure calculations, and improving the motion of the plasma electrons that collide with the atom.

Keywords: atomic structure; hartree fock; exchange; line broadening; scattering

0. Introduction

Calculation of atomic structure (energy eigenvalues and wavefunctions) of multi-electron atoms or molecules is complicated because no exact analytical solution exists. There are a variety of methods that were introduced to solve for multi-electron systems. The most-studied system being helium-like atoms [See survey in 1]. Probably the most far-reaching method is that of Hartree [2], who used an iterative-refinement method¹. The two-electron (non-relativistic) Hamiltonian is

$$H(r_1, r_2) = H_0(r_1) + H_0(r_2) + V(r_1, r_2) \quad (1)$$

$$\begin{aligned} H_0(r_1) &= -\frac{1}{2} \nabla_1^2 - \frac{Z}{r_1} \\ V(r_1, r_2) &= \frac{1}{|\vec{r}_1 - \vec{r}_2|}. \end{aligned} \quad (2)$$

¹ This method fails to capture some correlation effects because the potential in which the electron is moving is defined to be a mean field of the other electrons; which is to say that it does not account for the additional repulsion when the two electrons are close to each other.

Hartree can solve for the motion of one of the electrons by calculating average fields due to the second electron. The average field due to the second electron is defined as

$$\int_0^\infty d^3\vec{r}_2 \psi_2^*(r_2) \frac{1}{|\vec{r}_1 - \vec{r}_2|} \psi_2(r_2).$$

20 The Hartree method uses an iterative procedure to solve for the atomic structure by solving for the
21 motion of individual electrons with fields due to the other electrons. Each iteration improves the
22 wavefunction; this procedure is repeated until a desired convergence is reached. The steps of the
23 Hartree method can be summarized as

24 1) Assume a wavefunction for the state of interest (hydrogenic is good enough for this step)
25
26 2) Determine a mean-Coulomb field acting on electron i based on the wavefunctions of the other
27 $N - 1$ electrons.
28 3) Solve the one-electron Schrödinger equation for electron i in its mean-Coulomb field to generate
29 a new set of wavefunctions.
30 4) Repeat steps 2)-3) until convergence is achieved.

31 Hartree's method however, neglected the physical indistinguishability of identical particles;
32 this resulted in poor results in matching the helium spectrum. The two-electron Hamiltonian (Eq
33 1) is unchanged upon exchange of the positions of electron 1 and electron 2. The wavefunction
34 eigensolution, therefore must also have this property, such that

$$\Psi(\vec{r}_1, \vec{r}_2) = \pm \Psi(\vec{r}_2, \vec{r}_1), \quad (3)$$

$$= \frac{1}{\sqrt{2}} [\psi_1(\vec{r}_1)\psi_2(\vec{r}_2) \pm \psi_2(\vec{r}_1)\psi_1(\vec{r}_2)], \quad (4)$$

35 where ψ_1 and ψ_2 are the one-electron wavefunctions for electrons 1 and 2, respectively. For the case of
36 the non-relativisitic helium atom, the positive symmetry sign is interpreted as the spin-anti-aligned
37 case, while the anti-symmetry is the spin-aligned case.

38 The Hartree-Fock equations [1,3,4] are based on a variational method to minimize the energy
39 of the system using the fully symmetrized wavefunctions in Eq (4), resulting in the following set of
40 differential equations for ψ_1 and ψ_2 ,

$$\left[-\frac{1}{2} \nabla_1^2 - \frac{Z}{r_1} + V_C(r_1) - E \right] \psi_1(\vec{r}_1) \approx \mp \left\{ \int d^3\vec{r}_2 \psi_1(\vec{r}_2) \frac{1}{r_{12}} \psi_2(\vec{r}_2) \right\} \psi_2(\vec{r}_1) \quad (5)$$

$$\left[-\frac{1}{2} \nabla_2^2 - \frac{Z}{r_2} + V_C(r_2) - E \right] \psi_2(\vec{r}_2) \approx \mp \left\{ \int d^3\vec{r}_1 \psi_1(\vec{r}_1) \frac{1}{r_{12}} \psi_2(\vec{r}_1) \right\} \psi_1(\vec{r}_2) \quad (6)$$

for a two electron system; V_C is the average *direct* Coulomb potential from the other electron,

$$V_C(r_1) = \int_0^\infty d^3\vec{r}_2 \psi_2(\vec{r}_2) \frac{1}{r_{12}} \psi_2(\vec{r}_2),$$

41 and the terms in curly brackets on the right-hand side are the exchange terms. Here we have omitted
42 some of the overlap integrals, which are often approximated with Lagrangian multipliers [4]². The
43 Hartree-Fock equations are some of the most widely-used equations in atomic structure [1,4,5], often
44 providing an accurate set of starting wavefunctions and energies.

One source of uncertainty with solving the Hartree-Fock equations is the treatment of the exchange term on the right-hand sides of Eqns (5) and (6). Current calculations which treat exchange explicitly

² If the two wavefunctions are assumed to be orthogonal, then these terms vanish.

approximate these terms as if they are an inhomogeneous term of a differential equation [4,6–8], where the differential equation for electron 1 is approximated as

$$\left[-\frac{1}{2}\nabla_1^2 - \frac{Z}{r_1} + V_C(r_1) - E \right] \psi_1(\vec{r}_1) \approx \mp s(r_1), \quad (7)$$

where $s(r_1)$ is the inhomogeneous term of the differential equation, which contains the exchange term, and its evaluation relies on the previous guess of the new wavefunction for which we are trying to solve. In addition, one must be careful with evaluating an inhomogeneous term numerically [4].

Contrast Eq (7) with Eq (5), where the function that is being solved is inside the integral on the right-hand side, therefore the Hartree-Fock equations are integro-differential equations. Computing power has now reached a point where integro-differential equations can be solved using finite-difference matrices similar to the one used by Beck [8].

1. Finite Difference Matrix to Solve the Schrödinger Equation

Before we begin discussing solutions to the Hartree-Fock equations, we would like to introduce the idea of using matrices to solve the one-electron Schrödinger equation for a problem where the solution is known. We therefore choose to use finite-difference matrix method to solve for the hydrogen atom. The non-relativistic hydrogen wavefunction can be separated into a radial and spherical coordinates,

$$\psi(r, \theta, \phi) = \frac{1}{r} R_{nl}(r) Y_{lm}(\theta, \phi),$$

where the behavior of the angular part is known and well-characterized by the spherical harmonics, and the radial wavefunction, $R_{nl}(r)$ is the part that needs to be solved. The radial equation is the solution to the Schrödinger equation (atomic units used throughout; $\hbar = 1$, $m_e = 1$, and $e = 1$),

$$\left[-\frac{d^2}{dr^2} + \frac{l(l+1)}{r^2} - \frac{2Z}{r} \right] R_{nl}(r) = 2E_n R_{nl} \quad (8)$$

As is shown in Beck [8], the second-order derivative can be represented with finite-difference coefficients,

$$\begin{aligned} \left[\frac{d^2}{dr^2} R_{nl}(r_i) \right] &\approx \frac{1}{(\Delta r)^2} [R_{nl}(r_{i+1}) + R_{nl}(r_{i-1}) - 2R_{nl}(r_i)] \\ &\approx \frac{1}{(\Delta r)^2} (1 \quad -2 \quad 1) \begin{pmatrix} R_{nl}(r_{i-1}) \\ R_{nl}(r_i) \\ R_{nl}(r_{i+1}) \end{pmatrix} \end{aligned} \quad (9)$$

which can be written more generally as a matrix

$$\left[\frac{d^2}{dr^2} R_{nl}(r) \right] \approx \frac{1}{(\Delta r)^2} \begin{pmatrix} -2 & 1 & 0 & 0 & \dots \\ 1 & -2 & 1 & 0 & \dots \\ 0 & 1 & -2 & 1 & \dots \\ 0 & 0 & 1 & -2 & \dots \\ \vdots & \vdots & \vdots & \vdots & \ddots \end{pmatrix} \begin{pmatrix} R_{nl}(r_1) \\ R_{nl}(r_2) \\ R_{nl}(r_3) \\ R_{nl}(r_4) \\ \vdots \end{pmatrix}. \quad (10)$$

The potential in which the electron is moving is a diagonal matrix,

$$V(r)R_{nl}(r) = \begin{pmatrix} V(r_1) & 0 & 0 & 0 & \cdots \\ 0 & V(r_2) & 0 & 0 & \cdots \\ 0 & 0 & V(r_3) & 0 & \cdots \\ 0 & 0 & 0 & V(r_4) & \cdots \\ \vdots & \vdots & \vdots & \vdots & \ddots \end{pmatrix} \begin{pmatrix} R_{nl}(r_1) \\ R_{nl}(r_2) \\ R_{nl}(r_3) \\ R_{nl}(r_4) \\ \vdots \end{pmatrix}, \quad (11)$$

where $V(r)$ is

$$V(r) = \frac{l(l+1)}{r^2} - 2\frac{Z}{r}.$$

56 The total Hamiltonian will simply be the sum of the differential matrix and the potential matrix.
 57 These techniques are well established [e.g. 9,10] and could be improved upon by using higher-order
 58 finite-difference elements, or using the Numerov method in matrix form.

59 The advantage of this technique is that any linear-algebra package, such as LAPACK, can be used
 60 to diagonalize this Hamiltonian to get energies and wavefunctions. As a result, complications with
 61 shooting methods, such as trying to match the inner and outer solutions (or having to search for an
 62 eigenvalue), are avoided—though at a cost: numerically solving for the eigenvalues and eigenvectors
 63 of a large Hamiltonian can become time-consuming. As with any finite-difference method, smaller
 64 Δr results in more accurate wavefunctions, but requires a larger matrix to solve, which means the
 65 calculation will converge more slowly.

66 To illustrate the accuracy of the calculations using this method, table 1 shows the energy
 67 eigenvalues of hydrogen assuming a maximum r of 50 Bohr, and compares the accuracy of different
 68 Δr ; the Hamiltonians are $N \times N$ matrices where $N = 100, N = 250, N = 500, N = 1000$ for $\Delta r = 0.5$,
 69 $\Delta r = 0.2, \Delta r = 0.1, \Delta r = 0.05$, respectively (all in units of Bohr distance; 1 Bohr = 5.29×10^{-9} cm).
 We see that the errors in the energy eigenvalue for $\Delta r = 0.1$ Bohr is roughly 0.2% for the ground state,

Table 1. Numerical Eigenvalue Solutions

n	$\Delta r = 0.5$	$\Delta r = 0.2$	$\Delta r = 0.1$	$\Delta r = 0.05$	Exact
1	-0.94427	-0.99019	-0.99751	-0.99937	-1.00000
2	-0.24621	-0.24938	-0.24984	-0.24996	-0.25000
3	-0.11035	-0.11098	-0.11108	-0.11110	-0.11111
4	-0.06218	-0.06237	-0.06240	-0.06241	-0.06250

70 and less than 0.1% for the excited states, while the $\Delta r = 0.05$ Bohr calculation has 0.06% errors in the
 71 ground-state energies, and $\leq 0.02\%$ errors for the excited states.

73 2. Matrix form of the Hartree-Fock Equation

To solve for multi-electron systems, we can extend Eq (10) to solve for more than one radial function simultaneously. For example, one can construct a differential matrix for a wavefunction that has two coordinate positions,

$$R(r_i, r_j) = \begin{pmatrix} R(r_1, r_1) \\ R(r_2, r_1) \\ R(r_3, r_1) \\ \vdots \\ R(r_1, r_2) \\ R(r_2, r_2) \\ R(r_3, r_2) \\ \vdots \end{pmatrix}$$

⁷⁴ But this means that the vector size is N^2 instead of N . Therefore, the most practical method for solving
⁷⁵ for multi-electron systems is the Hartree-Fock equations—though it is not impossible to solve such a
⁷⁶ large system on a laptop computer³.

The Hartree-Fock equations (Eqns 5 and 6) contain two additional terms not present in the one-electron Schrödinger equation: the direct and exchange interactions with the other electrons in the system. For the rest of the section, we use the Taylor expansion of the Coulomb interaction,

$$\frac{1}{|\vec{r}_1 - \vec{r}_2|} = \sum_{k=0}^{\infty} \frac{r_<^k}{r_>^{k+1}} P_k(\cos \gamma_{12}) \quad (12)$$

⁷⁷ where $r_<$ and $r_>$ are the lesser/greater of r_1 and r_2 , and P_k is a Legendre polynomial, and $\cos \gamma_{12}$ is the
⁷⁸ angle that separates the two particles.

The direct term uses the spherically-averaged potential, which is just the monopole term. The i^{th} electron feels the average monopole interaction from the other electrons

$$V_{dir}(r) R_i(r) = R_i(r) \sum_{j \neq i} \int_0^{\infty} dr_1 R_j^*(r_1) R_j(r_1) \frac{1}{r_>} \quad (13)$$

where $r_>$ is the greater of r_1 and r . This poses no complications from the treatment in section 1 due to the fact that the resulting potential is diagonal like Eq (11), and can just be added to the centrifugal and nuclear potentials. The exchange term is a bit more complicated [1,4],

$$V_{exch}(r) \psi_i(\vec{r}) = \mp \sum_{j \neq i} \sum_k \psi_j(\vec{r}) \int_0^{\infty} d^3 \vec{r}_1 \psi_j^*(\vec{r}_1) \frac{r_<^k}{r_>^{k+1}} P_k(\cos \gamma) \psi_i(\vec{r}_1),$$

Use of the spherical harmonics, their relationship with the Wigner 3j-symbols, and averaging over all m quantum numbers, the exchange contribution can be reduced to [4],

$$V_{exch}(r) R_i(\vec{r}) = \sum_{j \neq i} \sum_k -\frac{1}{2} \begin{pmatrix} l_j & k & l_i \\ 0 & 0 & 0 \end{pmatrix}^2 R_j(\vec{r}) \int_0^{\infty} dr_1 R_j^*(r_1) \frac{r_<^k}{r_>^{k+1}} R_i(r_1). \quad (14)$$

We can define the integral with finite difference matrix coefficients in a similar way to the derivative, discussed in the previous section. The integral in Eq (14) can be discretized as follows (where the coordinates r and r_1 have been replaced with a spatial index, r_x and r_y respectively),

$$V(r_x) \propto \sum_{j \neq i} \sum_k R_j(r_x) \sum_y R_j^*(r_y) \hat{V}^k(r_x, r_y) R_i(r_y) \Delta r_y.$$

which can be written as a matrix (omitting the sums over j and k),

$$\Delta r \begin{pmatrix} R_j(r_1) R_j^*(r_1) \hat{V}^k(r_1, r_1) & R_j(r_1) R_j^*(r_2) \hat{V}^k(r_1, r_2) & R_j(r_1) R_j^*(r_3) \hat{V}^k(r_1, r_3) & \cdots \\ R_j(r_2) R_j^*(r_1) \hat{V}^k(r_2, r_1) & R_j(r_2) R_j^*(r_2) \hat{V}^k(r_2, r_2) & R_j(r_2) R_j^*(r_3) \hat{V}^k(r_2, r_3) & \cdots \\ R_j(r_3) R_j^*(r_1) \hat{V}^k(r_3, r_1) & R_j(r_3) R_j^*(r_2) \hat{V}^k(r_3, r_2) & R_j(r_3) R_j^*(r_3) \hat{V}^k(r_3, r_3) & \cdots \\ R_j(r_4) R_j^*(r_1) \hat{V}^k(r_4, r_1) & R_j(r_4) R_j^*(r_2) \hat{V}^k(r_4, r_2) & R_j(r_4) R_j^*(r_3) \hat{V}^k(r_4, r_3) & \cdots \\ \vdots & \vdots & \vdots & \ddots \end{pmatrix} \begin{pmatrix} R_i(r_1) \\ R_i(r_2) \\ R_i(r_3) \\ R_i(r_4) \\ \vdots \end{pmatrix}. \quad (15)$$

³ In fact, radial solutions of three-electron problems can be solved on a laptop with the help of sparse matrix eigenvalue solvers. Any system larger than this would require the use of a supercomputer.

79 This method still requires knowledge of the other electrons, but now this equation solves for $R_i(r)$
 80 once per iteration. Contrast this with the inhomogeneous differential equation method, where each
 81 iteration on the wavefunction requires repeated integrations of the Hartree-Fock equations to accurately
 82 calculate the effect of exchange.

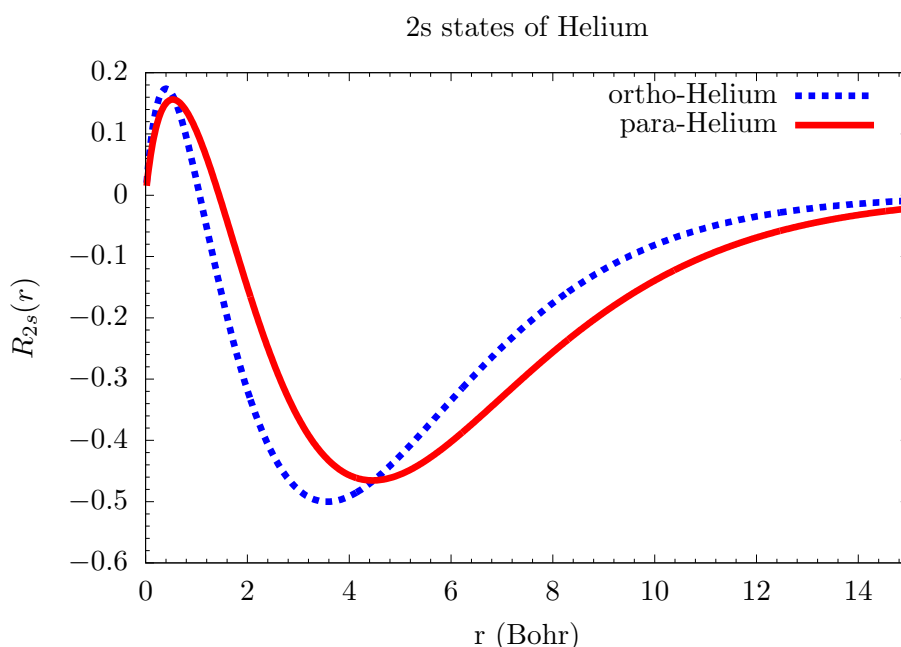


Figure 1. Numerical Results of using exact matrix exchange method.

83 The numerical results of using this Hartree-Fock matrix method are plotted in figure 1 for the
 84 spin-aligned (ortho-helium) and spin-anti-aligned (para-helium) cases. These results differ from the
 85 Cowan wavefunctions, even for the average (of para- and ortho-helium). The biggest difference is
 86 in the size of the part that overlaps with the center electron, as evident in figure 2. This means that
 87 Cowan's code predicts a wavefunction that is more likely to occupy the same space as the 1s electron.
 88 Orthogonality between the 1s and 2s electrons offers a useful metric for comparison. Cowan's code
 89 uses Lagrangian multipliers to force orthogonality (meaning that overlap integrals with non-identical
 90 electrons are zero) between the 1s and 2s electrons. Our calculation of LS-averaged wavefunctions
 91 produce overlap integrals for the 2s and 1s states that are 0.02. But if we calculate each LS term
 92 (ortho- and para-helium), the 1s and 2s ortho-helium (spin-aligned) triplet states have overlap integrals
 93 that are less than 0.001—comparable to the Cowan code, but the 1s and 2s states of the para-helium
 94 singlet state are not orthogonal (overlap integral is 0.08); this has been observed before in Hartree-Fock
 95 calculations [3,11].

96 The energies are also different—and this may be where these details matter most. In Table 2,
 97 we compare the different calculations for the energy separation of the two different LS terms (para-
 98 and ortho-helium) of the 2s state of helium to the reference value from NIST [12,13]. Our matrix
 99 Hartree-Fock method gives a value that is nearly 10% lower than that predicted by Cowan and in
 100 much better agreement with the reference value. A direct numerical two-electron solution (where we
 101 expand Eq (10) to two dimensions and include a monopolar repulsion term; this is *not* the Hartree-Fock
 102 equations) agrees well with the reference value.

Table 2. Energy difference between $2s^3S$ and $2s^1S$ in Ry

Cowan	Hartree-Fock with Exact Exchange	Direct Two-Electron Solution	Measured [12,13]
0.06749	0.06158	0.0602	0.05857

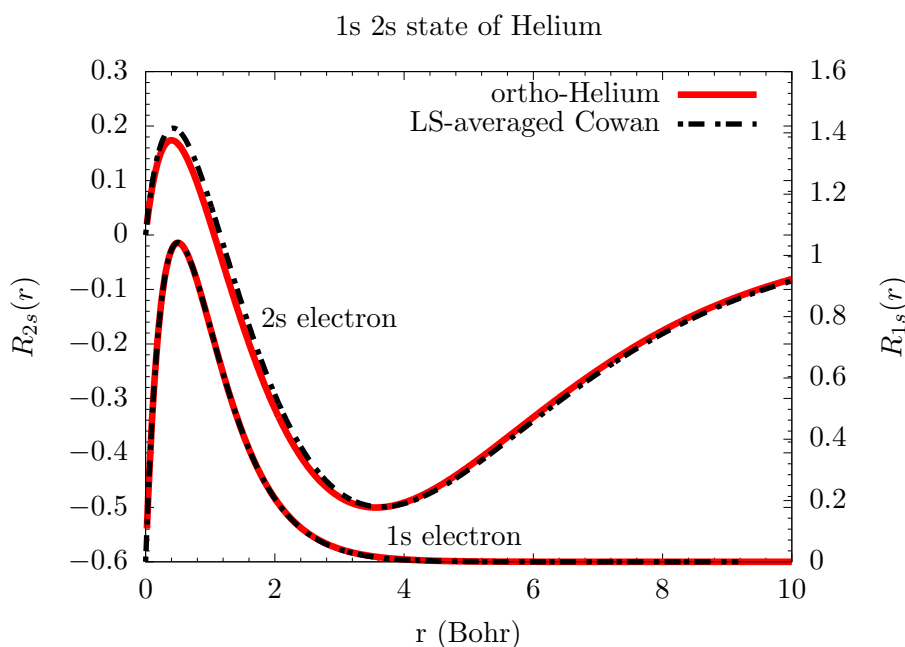


Figure 2. The ortho-helium wavefunctions compared with Cowan's 1s 2s wavefunction. The new calculations with exact exchange are given in red, while Cowan's calculation are in dot-dashed black lines.

¹⁰³ **3. Extension to Free-Electron Wavefunctions**

This same technique can also be used to calculate free-electron wavefunctions. However, the problem is slightly different than the bound-electron problem. First, the eigenvalue is known, and second, the outer boundary condition is not zero. To accommodate this, we move the energy ($E = \frac{1}{2}k^2$) to the other side of Eq (8), so that the system for which we are solving is

$$(H - E)\psi(r) = 0$$

We then use a matrix solver ($Ax = b$), rather than an eigenvalue solver and set the b vector equal to zero except for the final value, which is set to 1,

$$b = \begin{pmatrix} 0 \\ 0 \\ 0 \\ \vdots \\ 0 \\ 1 \end{pmatrix}.$$

¹⁰⁴ This will ensure that the wavefunction does not decay to zero at the outer-most boundary.

¹⁰⁵ The changes in the free-electron wavefunction are shown in figures 3 and 4 for a distorted-wave
¹⁰⁶ treatment, where we assume that the atom is not perturbed by the presence of the free-electron.
¹⁰⁷ Figure 3 shows the free electron reacting to a hydrogen atom in the 2s state, while figure 4 shows the
¹⁰⁸ free-electron reacting to a lithium atom in the 1s²2s configuration. In these figures, we also plot the
¹⁰⁹ plane-wave solution for the same k state, and a local-density-approximation (LDA) for the exchange
¹¹⁰ contribution [4,14,15]. The changes in the wavefunction in figure 3 are fairly minor, and the LDA giving
¹¹¹ a fairly reasonable amplitudes for the inner 5 Bohr of the wavefunction. The lithium wavefunctions

112 calculated with an LDA, on the other hand, are not nearly as good, the amplitudes of the exact exchange
 113 are lower by 30-50%. This means that if one were trying to accurately calculate the effects of penetrating
 114 collisions for multi-electron—meaning more than one electron—systems, the LDA wavefunction may
 115 not be accurate enough depending on the application.

116 The differences between the three treatments (Coulomb/Plane wave, LDA, and exact exchange)
 117 become less important as the charge of the atom increases. For example, in Li-like boron, the differences
 118 are much less pronounced because the nuclear charge becomes the dominant contribution to the
 119 potential.

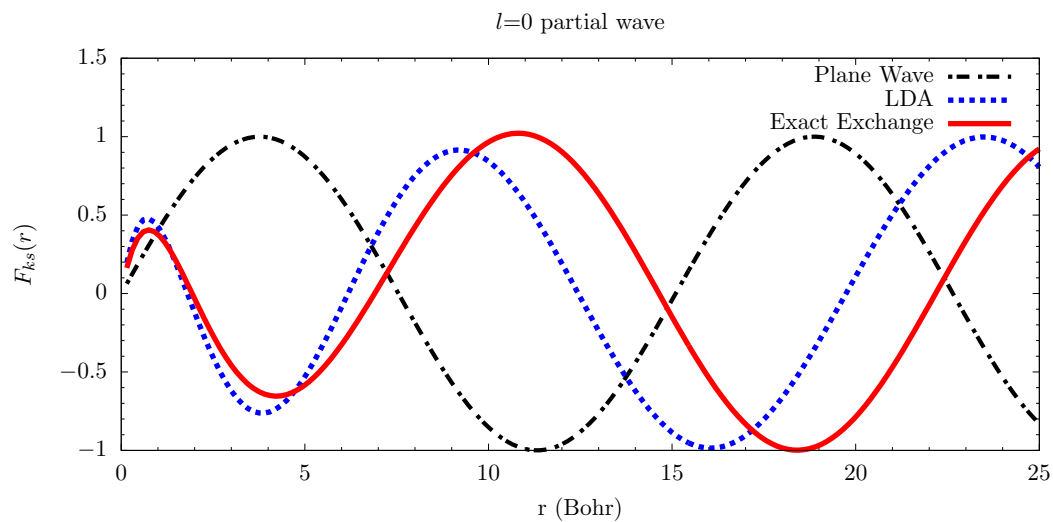


Figure 3. The $l = 0$ partial wave of the free-electron wavefunction under different approximations. Black dot dashed is the plane wave, dotted blue is using an LDA to approximate the exchange correlations, and solid red is the exact exchange treatment. The states are reacting to the presence of a hydrogen atom in the 2s state

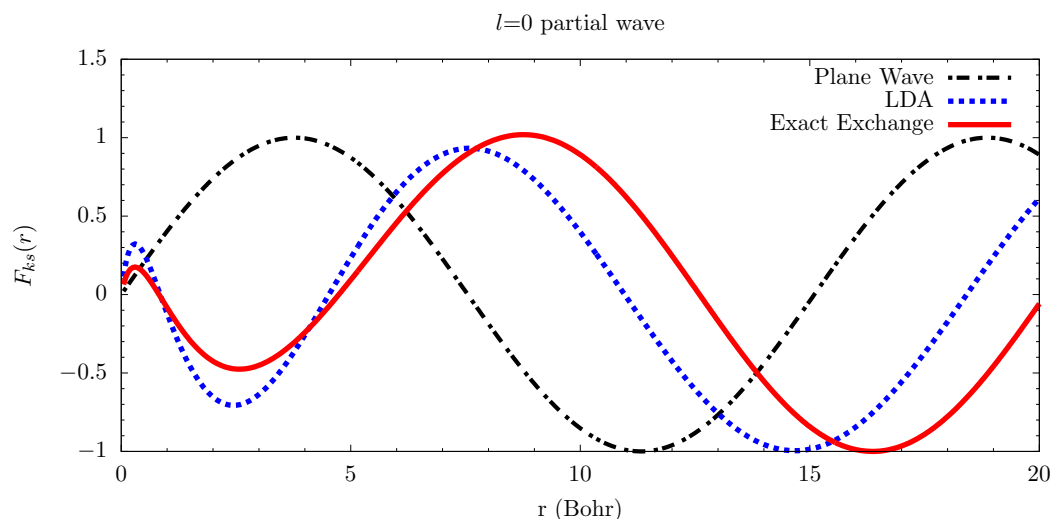


Figure 4. Same as figure 3, but reacting to the Li $1s^2 2s$ state.

120 4. Application To Spectral Line Broadening

121 The line broadening of spectral lines is due to the radiator interacting with its environment.
122 Therefore the accuracy of spectral line broadening depends on three primary details: the atomic
123 structure, the description of the plasma ensemble properties, and the way the plasma and atoms
124 interact. The work here has an impact on spectral line broadening in two ways: the atomic structure
125 and the behavior of plasma electrons when they impact the radiator.

126 The changes in the atomic data will affect all spectral line shape calculations. All spectral line
127 broadening calculations require input from an atomic structure code, and the most commonly-used
128 information is the energy levels and dipole moments. As we showed in section 2, the energy levels of
129 the helium atom can substantially change with a different treatment of exchange. The small changes in
130 the wavefunctions will also result in changes in the dipole moments used by line-shape codes.

131 In addition, there are a few calculations which treat the plasma electron quantum mechanically.
132 Regardless of the method (second-order distorted-wave method [16,17], or a CCC method [18–22]),
133 these calculations require a set of starting wavefunctions for the plasma electrons. Most of these
134 methods use LDA methods for exchange, but as demonstrated in the previous sections, these may not
135 be the most accurate when exchange becomes important. This method of using an exact exchange
136 treatment is now being implemented in the DWE line shape code [23,24] (which was used in the
137 SLSP4 workshop), which improves upon the relaxation theory method of Junkel *et al.* [25] to include
138 exchange.

139 Calculations which treat penetration effects explicitly in electron broadening have to take into
140 account two processes: the softening of the potential when the plasma electrons occupy the same space
141 as the bound electron, and exchange. Exchange calculations are extremely difficult to perform if the
142 bound- and free-electron wavefunctions are not orthogonal, and become considerably simpler when
143 the wavefunctions are orthogonal. LDA methods do not guarantee orthogonality, while these matrix
144 methods can achieve orthogonality to one part in 1000, thus simplifying exchange calculations.

145 5. Summary

146 We present a different technique for evaluating exchange effects in multi-electron atoms and
147 in collision processes. Rather than treating the exchange term of the Hartree-Fock equations as
148 an inhomogeneous term of the differential equation, we treat it explicitly as an integro-differential
149 equation. We have written the exchange integral as a matrix, and then approximating the rest of
150 the Hamiltonian terms as finite-difference coefficients, we can use linear algebra packages such as
151 LAPACK to diagonalize the total Hamiltonian to get the energies and wavefunctions. This method can
152 be used for either bound-state, or free-state systems. These lead to some differences in the evaluation of
153 the helium atom energy-level structure and wavefunctions. The behavior of penetrating free electrons
154 near the origin is differs from the LDA treatment of exchange for multi-electron systems, and can lead
155 to changes in the broadening of these systems.

156 Acknowledgments:

157 T.A.G. acknowledges support from the National Science Foundation Graduate Research
158 Fellowship under grant DGE-1110007. M.H.M., and D.E.W. acknowledge support from the United
159 States Department of Energy under grant DE-SC0010623, the Wooton Center for Astrophysical Plasma
160 Properties under the United States Department of Energy under grant DE-FOA-0001634, and the
161 National Science Foundation grant NSF-AST 1707419. Sandia National Laboratories is a multimission
162 laboratory managed and operated by National Technology and Engineering Solutions of Sandia, LLC.,
163 a wholly owned subsidiary of Honeywell International, Inc., for the U.S. Department of Energy's
164 National Nuclear Security Administration under contract DE-NA-0003525. T.A.G. and S.B.H. was also
165 supported by the U.S. Department of Energy, Office of Science Early Career Research Program, Office
166 of Fusion Energy Sciences under FWP-14-017426. We thank Dr. Chris Fontes, Dr. Andrew Baczewski,
167 and Dr. Daniel Jensen for stimulating discussions.

168 **References**

- 169 1. Bethe, H.A.; Salpeter, E.E. *Quantum Mechanics of One- and Two-Electron Atoms*; 1957.
- 170 2. Hartree, D.R. The Wave Mechanics of an Atom with a Non-Coulomb Central Field. Part I. Theory and
171 Methods. *Proceedings of the Cambridge Philosophical Society* **1928**, *24*, 89.
- 172 3. Fock, V. Näherungsmethode zur Lösung des quantenmechanischen Mehrkörperproblems. *Zeitschrift für
173 Physik* **1930**, *61*, 126–148.
- 174 4. Cowan, R.D. *The theory of atomic structure and spectra*; 1981.
- 175 5. Grant, I.P. *Relativistic Quantum Theory of Atoms and Molecules*; 2007.
- 176 6. Talman, J.D.; Shadwick, W.F. Optimized effective atomic central potential. *Phys. Rev. A* **1976**, *14*, 36–40.
- 177 7. Shiozaki, T.; Hirata, S. Grid-based numerical Hartree-Fock solutions of polyatomic molecules. *Phys. Rev. A*
178 **2007**, *76*, 040503.
- 179 8. Beck, T.L. Real-space mesh techniques in density-functional theory. *Reviews of Modern Physics* **2000**,
180 *72*, 1041–1080, [cond-mat/0006239].
- 181 9. Chow, P.C. Computer Solutions to the Schrödinger Equation. *American Journal of Physics* **1972**, *40*, 730–734.
- 182 10. Pillai, M.; Goglio, J.; Walker, T.G. Matrix Numerov Method for solving Schrödinger's equation. *American
183 Journal of Physics* **2012**, *80*, 1017–1019.
- 184 11. Sharma, C.S. On the Hartree-Fock equations for helium with non-orthogonal orbitals. *Journal of Physics B:
185 Atomic and Molecular Physics* **1968**, *1*, 1023.
- 186 12. Kramida, A.; Yu. Ralchenko.; Reader, J.; and NIST ASD Team. NIST Atomic Spectra Database (ver. 5.5.2),
187 [Online]. Available: <https://physics.nist.gov/asd> [2015, April 16]. National Institute of Standards and
188 Technology, Gaithersburg, MD., 2018.
- 189 13. Morton, D.C.; Wu, Q.X.; Drake, G.W.F. Energy levels for the stable isotopes of atomic helium (He-4 I and
190 He-3 I). *Canadian Journal of Physics* **2006**, *84*, 83–105.
- 191 14. Slater, J.C. A Simplification of the Hartree-Fock Method. *Physical Review* **1951**, *81*, 385–390.
- 192 15. Kohn, W.; Sham, L.J. Self-Consistent Equations Including Exchange and Correlation Effects. *Physical
193 Review* **1965**, *140*, 1133–1138.
- 194 16. Madison, D.H.; Bray, I.; McCarthy, I.E. Exact second-order distorted-wave calculation for hydrogen
195 including second-order exchange. *Journal of Physics B Atomic Molecular Physics* **1991**, *24*, 3861–3888.
- 196 17. Kingston, A.E.; Walters, H.R.J. Electron scattering by atomic hydrogen - The distorted-wave second Born
197 approximation. *Journal of Physics B Atomic Molecular Physics* **1980**, *13*, 4633–4662.
- 198 18. Bray, I. Convergent close-coupling method for the calculation of electron scattering on hydrogenlike
199 targets. *Phys. Rev. A* **1994**, *49*, 1066–1082.
- 200 19. Bray, I.; Stelbovics, A.T. Calculation of Electron Scattering on Hydrogenic Targets. *Advances in Atomic
201 Molecular and Optical Physics* **1995**, *35*, 209–254.
- 202 20. Griem, H.R.; Ralchenko, Y.V.; Bray, I. Stark broadening of the B III 2s-2p lines. *Phys. Rev. E* **1997**,
203 *56*, 7186–7192.
- 204 21. Seaton, M.J. Atomic data for opacity calculations. XIII - Line profiles for transitions in hydrogenic ions.
205 *Journal of Physics B Atomic Molecular Physics* **1990**, *23*, 3255–3296.
- 206 22. Seaton, M.J.; Yan, Y.; Mihalas, D.; Pradhan, A.K. Opacities for Stellar Envelopes. *Mon. Not. Ro. Astr. Soc.*
207 **1994**, *266*, 805.
- 208 23. Gomez, T.A. Improving Calculations of the Interaction Between Atoms and Plasma Particles and its Effect
209 on Spectral Line Shapes. PhD thesis, University of Texas at Austin, 2017.
- 210 24. Gomez, T.A.; Nagayama, T.; Kilcrease, D.P.; Fontes, C.J.; Iglesias, C.A.; Lee, R.W.; Hansen, S.B.; Montgomery,
211 M.H.; Winget, D.E. Penetrating Collisions by Electrons and its Effect on Electron Broadening. *in prep* **2018**.
- 212 25. Junkel, G.C.; Gunderson, M.A.; Hooper, Jr., C.F.; Haynes, Jr., D.A. Full Coulomb calculation of Stark
213 broadened spectra from multielectron ions: A focus on the dense plasma line shift. *Phys. Rev. E* **2000**,
214 *62*, 5584–5593.